Cartilage-specific deletion of Mig-6 results in osteoarthritis-like disorder with excessive articular chondrocyte proliferation

Ben Staal[a], Bart O. Williams[b], Frank Beier[c], George F. Vande Woude[a,1], and Yu-Wen Zhang[a,1]

[a]Laboratory of Molecular Oncology, Center for Cancer and Cell Biology, Van Andel Research Institute, Grand Rapids, MI 49503; [b]Laboratory of Cell Signaling and Carcinogenesis, Center for Skeletal Disease and Tumor Metastasis, Van Andel Research Institute, Grand Rapids, MI 49503; and [c]Department of Physiology and Pharmacology, Western University, London, ON, Canada N6A 5C1

Contributed by George F. Vande Woude, January 15, 2014 (sent for review October 22, 2013)

A deficiency of mitogen-inducible gene-6 (Mig-6) in mice leads to the development of an early-onset, osteoarthritis (OA)-like disorder in multiple synovial joints, underlying its importance in maintaining joint homeostasis. Here we determined what joint tissues Mig-6 is expressed in and what role chondrocytes play in the Mig-6–deficient OA-like disorder. A Mig-6/lacZ reporter mouse strain expressing β-galactosidase under the control of the *Mig-6* gene promoter was generated to determine Mig-6 expression in joint tissues. By β-galactosidase staining, we demonstrated that Mig-6 was uniquely expressed in the cells across the entire surface of the synovial joint cavity, including chondrocytes in the superficial zone of articular cartilage and in the meniscus, as well as synovial lining cells. By crossing Mig-6–floxed mice to *Col2a1-Cre* transgenic mice, to generate cartilage-specific deletion of *Mig-6*, we demonstrated that deficiency of Mig-6 in the chondrocytes results in a joint phenotype that only partially recapitulates the OA-like disorder of the Mig-6–deficient mice: Ubiquitous deletion of Mig-6 led to the OA-like disorder in multiple joints, whereas cartilage-specific deletion affected the knees but rarely other joints. Furthermore, chondrocytes with Mig-6 deficiency showed excessive proliferative activities along with enhanced EGF receptor signaling in the articular cartilage and in the abnormally formed osteophytes. Our findings provide insight into the crucial requirement for Mig-6 in maintaining joint homeostasis and in regulating chondrocyte activities in the synovial joints. Our data also suggest that other cell types are required for fully developing the Mig-6–deficient OA-like disorder.

Gene 33 | Errfi1 | RALT | EGFR

Mitogen-inducible gene-6 (*Mig-6*) is an immediate early response gene encoding a scaffolding adaptor protein which fine-tunes receptor tyrosine kinase (RTK) signaling such as that of epidermal growth factor receptor (EGFR) and MET (1, 2). Its expression can be induced by growth factors including epidermal growth factor (EGF) and transforming growth factor alpha (TGF-α), as well as by many forms of stress stimuli, such as mechanical force (1). Mig-6 is best known for its ability to attenuate EGFR signaling via a negative feedback loop by interacting with EGFR and its downstream signaling molecules (3–7). It may function as a tumor suppressor and play roles in developmental and physiological processes such as skin morphogenesis and lung development (8–10). Mig-6 plays an essential role in the postnatal synovial joints: Mice with a Mig-6 deficiency develop early-onset osteoarthritis (OA)-like disorder in the knee, ankle, and temporal-mandibular joint (TMJ) (11). An increase of Mig-6 expression is found in canine osteoarthritic cartilage (12, 13); this is likely due to activation of certain growth factor signaling and/or mechanical stress that induces the expression of Mig-6 for protecting joint integrity. These data underline the importance of Mig-6 in maintaining joint homeostasis, and also indicate a potentially crucial role for Mig-6 in OA pathogenesis.

OA is the most common form of joint disease in humans (14), and can be triggered and influenced by diverse factors (15–17). Nonetheless, the mechanism underlying OA onset and progression is still poorly understood. The core pathological changes in OA include articular cartilage degradation and formation of osteophyte (also known as bony outgrowth) and subchondral cysts (17–20), which can all be observed in the Mig-6–deficient synovial joints (11). Chondrocytes in the articular cartilage synthesize many cartilage proteins for building the extracellular matrix (ECM) network that is responsible for withstanding biomechanical force. They also secrete various anabolic and catabolic cytokines or growth factors, as well as diverse proteases such as matrix metalloproteinases, for ECM remodeling, thereby maintaining a healthy and elastic cartilage structure (20). An imbalance of those chondrocyte-derived factors may impose an unwanted turnover of the ECM, leading to the breakdown of the cartilage structure and thus to OA (20). Besides chondrocytes, many other cells in the synovial joints may also participate in the pathogenesis of OA (17).

In this study, we determined what cells in the joint tissues express Mig-6 and what role chondrocytes may play in developing a Mig-6–deficient OA-like phenotype. For determining Mig-6 expression in joint tissues by β-galactosidase staining, we generated a Mig-6/lacZ reporter mouse strain that expressed β-galactosidase under the control of the *Mig-6* gene promoter. We crossed Mig-6–floxed mice to *Col2a1-Cre* transgenic mice (21) for the conditional deletion of *Mig-6* in chondrocytes, and determined how chondrocytes participate in the pathogenesis of the Mig-6–deficient OA-like disorder.

Significance

Mitogen-inducible gene 6 (Mig-6) was found to be an important factor in maintaining joint homeostasis, and its loss in mice results in the development of an osteoarthritis (OA)-like disorder in multiple synovial joints. However, it was unclear in what cells Mig-6 was expressed and what cells were causal for developing the OA-like phenotype. Here we report that Mig-6 is uniquely expressed in the cells surrounding entire surface of the synovial joint, including chondrocytes in the superficial zone of the articular cartilage and in the meniscus, and synovial lining cells. We found that although chondrocytes play a critical role in developing the OA-like disorder in the knees, other cell types are likely required for full development of the Mig-6–deficient joint phenotype.

Author contributions: G.F.V.W. and Y.-W.Z. designed research; B.S. and Y.-W.Z. performed research; B.S. and Y.-W.Z. analyzed data; B.O.W. and F.B. contributed new reagents/analytic tools; and Y.-W.Z. wrote the paper.

The authors declare no conflict of interest.

[1]To whom correspondence should be addressed. E-mail: YuWen.Zhang@vai.org or george.vandewoude@vai.org.

This article contains supporting information online at www.pnas.org/lookup/suppl/doi:10.1073/pnas.1400744111/-/DCSupplemental.

Results

Generation of Mig-6/lacZ Reporter Mice. Mig-6 deficiency in mice leads to the development of OA-like disorder in multiple synovial joints (11), but the origin of the cells causing this phenotype are not yet known. Identifying the cells expressing Mig-6 will be a key to understanding the mechanism underlying OA onset and progression. To determine where and when Mig-6 is expressed in the synovial joints, we engineered a mouse strain in which the β-galactosidase (lacZ reporter) was inserted into the *Mig-6* gene locus under the control of the *Mig-6* promoter (*Mig-6/lacZ* allele) (Fig. 1*A*). For both ES clones and Mig-6/lacZ reporter mice, allele-specific PCR was performed to confirm the proper homologous recombination between the targeting vector and the wild-type allele of *Mig-6* (Fig. 1*B*). Both the p1–p2 and p3–p8 primer pairs are specific for the *Mig-6/lacZ* allele, and amplification was observed in the $Mig\text{-}6^{lacZ/+}$ and $Mig\text{-}6^{lacZ/lacZ}$ ES clones and mice, but not in the wild-type ($Mig\text{-}6^{+/+}$) (Fig. 1*B*).

We then performed β-galactosidase staining to reveal the lacZ reporter activity, which is the indication of Mig-6 expression in the cells. The lacZ reporter activity was detected in the day-16 joints of $Mig\text{-}6^{lacZ/lacZ}$ embryo (Fig. 1*C*). A similar staining pattern was also observed in the 2-wk-old knee joints of $Mig\text{-}6^{lacZ/+}$ mouse (Fig. 1*D*). Specifically, the cells with high lacZ activity cover the entire surface of the joint cavity, including the chondrocytes in the superficial zone of articular cartilage and in the surface layer of meniscus, as well as the synovial lining cells (Fig. 1*E*). In the articular cartilage, the intensity of the lacZ staining decreased dramatically for chondrocytes in the middle zone and almost undetected in the deep zone (Fig. 1*E*). These data indicate that Mig-6 is uniquely expressed in the cells across the surface of joint cavity to maintain joint homeostasis, and losing Mig-6 activity in some or all of these cells is likely responsible for developing the OA-like phenotype (11).

Generation of Mig-6–Floxed Mice. To determine which cell type is causal for the osteoarthritic phenotype in $Mig\text{-}6^{-/-}$ joints (11), we generated another Mig-6 mouse strain that carried flox alleles for tissue-specific deletion of *Mig-6* (Fig. 2*A*). To generate the Mig-6–floxed mice, we first established ES cells carrying the targeted allele ($Mig\text{-}6^{Tar/+}$) and generated $Mig\text{-}6^{Tar/+}$ mice (Fig. 2 *A* and *B*). Both ES cells and mice carrying the targeted alleles were confirmed by allele-specific PCR to assure proper homologous recombination. Both p1–p2 and p3–p4 primer pairs, for the 5′ and 3′ homologous recombination respectively, specifically amplified the targeted alleles ($Mig\text{-}6^{Tar/+}$ and $Mig\text{-}6^{Tar/Tar}$) but not the wild type ($Mig\text{-}6^{+/+}$) (Fig. 2*B*).

We then crossed $Mig\text{-}6^{Tar/+}$ mice to FLPeR mice expressing Flp recombinase (22) to generate $Mig\text{-}6^{Tar/+};Flp^{tg/+}$ mice. The Flp recombinase excised the PGK-NEO cassette by recognizing the two flanking Flippase recognition target (FRT) sequences, resulting in the generation of *Mig-6–flox* allele (Fig. 2*A*). The success of PGK-NEO excision was confirmed by PCR using p5–p9 primer pair, which specifically amplified the targeted allele ($Mig\text{-}6^{Tar/+}$) but not the floxed allele ($Mig\text{-}6^{flox/flox}$ and $Mig\text{-}6^{flox/+}$) (Fig. 2*C*). Because the floxed alleles are carried in the germ line, we inbred the $Mig\text{-}6^{flox/flox};Flp^{tg/+}$ mice to establish the Mig-6–floxed mice without the *Flp* transgene ($Mig\text{-}6^{flox/flox}$), which were used for tissue-specific deletion of *Mig-6*.

To make sure that the floxed allele worked properly, we crossed $Mig\text{-}6^{flox/flox}$ mice to the *CMV-Cre* transgenic mice ubiquitously expressing Cre recombinase (23), which recognizes the two LoxP sites for the deletion of the *Mig-6* exons 2–4. Complete deletion of *Mig-6* was confirmed in the $Mig\text{-}6^{\Delta/\Delta};CMV^{Cre}$ mouse, as Mig-6 expression was not detected in the tissues derived from the $Mig\text{-}6^{\Delta/\Delta};CMV^{cre}$ mouse but in those of control one ($Mig\text{-}6^{+/+};CMV^{cre}$) (Fig. 2 *D* and *E*). Moreover, the $Mig\text{-}6^{\Delta/\Delta};CMV^{Cre}$ mice developed OA-like disorder in multiple synovial joints, including the knee, ankle, and TMJ, recapitulating the joint phenotype observed in the $Mig\text{-}6^{-/-}$ mice (Figs. 2 and 3).

Development of OA-Like Disorder in Knee Joints with Cartilage-Specific Deletion of *Mig-6*. Because Mig-6 expression was high in the chondrocytes in the articular cartilage and meniscus, we asked whether they were the cells causing the pathological changes in Mig-6–deficient joints. We crossed $Mig\text{-}6^{flox/flox}$ mice to *Col2a1-Cre* transgenic mice (21) to generate $Mig\text{-}6^{flox/flox};Col2a1^{Cre}$ mice, in which *Mig-6* is deleted in the chondrogenic cells (Fig. 3*A*). Whereas the majority of the Mig-6–deficient mice ($Mig\text{-}6^{-/-}$ and $Mig\text{-}6^{\Delta/\Delta};CMV^{Cre}$) died within 6 mo of age (11), $Mig\text{-}6^{flox/flox};Col2a1^{Cre}$ mice lived much longer, with the majority living more than a year. Histopathologically, we observed osteoarthritic changes in the knee joints of $Mig\text{-}6^{flox/flox};Col2a1^{Cre}$ mice from ages of 3 mo to over 1 y, indicating that chondrocytes do play a role in developing Mig-6–deficient OA-like disorder in their knee joints. These pathological abnormalities, including osteophytes, articular cartilage degradation, and subchondral cyst formation (Fig. 3*B*), were similar to those observed in the knee joints of $Mig\text{-}6^{-/-}$ (11) and $Mig\text{-}6^{\Delta/\Delta};CMV^{Cre}$ mice (Fig. 2*F*).

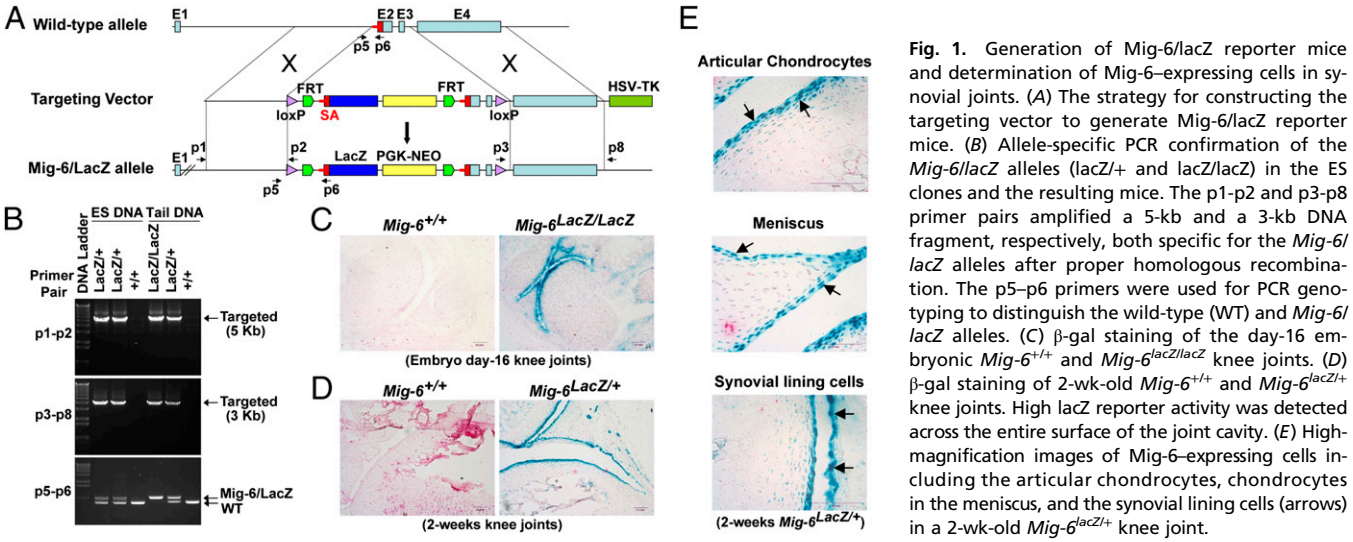

Fig. 1. Generation of Mig-6/lacZ reporter mice and determination of Mig-6–expressing cells in synovial joints. (*A*) The strategy for constructing the targeting vector to generate Mig-6/lacZ reporter mice. (*B*) Allele-specific PCR confirmation of the *Mig-6/lacZ* alleles (lacZ/+ and lacZ/lacZ) in the ES clones and the resulting mice. The p1-p2 and p3-p8 primer pairs amplified a 5-kb and a 3-kb DNA fragment, respectively, both specific for the *Mig-6/lacZ* alleles after proper homologous recombination. The p5–p6 primers were used for PCR genotyping to distinguish the wild-type (WT) and *Mig-6/lacZ* alleles. (*C*) β-gal staining of the day-16 embryonic $Mig\text{-}6^{+/+}$ and $Mig\text{-}6^{lacZ/lacZ}$ knee joints. (*D*) β-gal staining of 2-wk-old $Mig\text{-}6^{+/+}$ and $Mig\text{-}6^{lacZ/+}$ knee joints. High lacZ reporter activity was detected across the entire surface of the joint cavity. (*E*) High-magnification images of Mig-6–expressing cells including the articular chondrocytes, chondrocytes in the meniscus, and the synovial lining cells (arrows) in a 2-wk-old $Mig\text{-}6^{lacZ/+}$ knee joint.

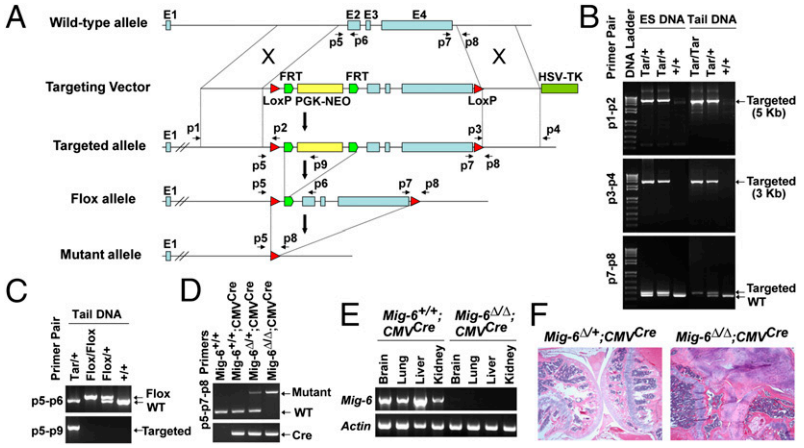

Fig. 2. Generation and characterization of Mig-6–floxed mice. (*A*) The strategy for the generation of Mig-6–floxed mice. (*B*) Confirmation of proper homologous recombination by allele-specific PCR. Genomic DNA from ES clones and the resulting mice was used for PCR amplification with primer pairs (p1–p2 and p3–p4) specific for the targeted alleles (Tar/+ and Tar/Tar). The p7–p8 primer pair was used for distinguishing between WT and the targeted allele. (*C*) PCR confirmation of the *Mig-6–flox* allele using mouse tail DNA. The p5–p9 primers specifically amplified the targeted allele, whereas the p5–p6 pair separated the WT and floxed alleles. (*D*) Deletion of Mig-6 in *Mig-6*$^{\Delta/\Delta}$;*CMV*^{Cre} mice by crossing Mig-6–floxed mice to CMV-cre mice. The p5–p8 primers detected the mutant alleles (*Mig-6*$^{\Delta/\Delta}$ and *Mig-6*$^{\Delta/+}$), and the p7–p8 pair detected the WT allele. The presence of CMV-Cre was determined by Cre-specific PCR. (*E*) RT-PCR detection of Mig-6 expression in the tissues of the *Mig-6*$^{+/+}$;*CMV*^{Cre} and *Mig-6*$^{\Delta/\Delta}$;*CMV*^{Cre} mice. Actin was used as an internal control. (*F*) Knee joints from 3.6-mo-old *Mig-6*$^{\Delta/+}$;*CMV*^{Cre} and *Mig-6*$^{\Delta/\Delta}$;*CMV*^{Cre} mice; *Mig-6*$^{\Delta/\Delta}$;*CMV*^{Cre} mice developed OA-like disorder, phenocopying *Mig-6*$^{-/-}$ mice.

To our surprise, other synovial joints such as the ankle and TMJ were rarely affected in the *Mig-6*$^{flox/flox}$;*Col2a1*^{Cre} mice (Fig. 3 *C* and *D*). Even after 15 mo of age, we rarely found osteophyte formation in the ankles of *Mig-6*$^{flox/flox}$;*Col2a1*^{Cre} mice, but the ankles of *Mig-6*$^{\Delta/\Delta}$;*CMV*^{Cre} mice showed extensive changes (swelling, stiffness, osteophytes, etc.) (Fig. 3*C*), resembling those found in *Mig-6*$^{-/-}$ mice (11). The rarity of OA-like penetration in the TMJ (Fig. 3*D*) likely explains why the majority of *Mig-6*$^{flox/flox}$;*Col2a1*^{Cre} mice can live much longer than the Mig-6–deficient mice (11). These data suggest that, although chondrocytes play a role in developing OA-like disorder in the Mig-6–deficient knee joint, other cell types are likely responsible for fully developing the Mig-6–deficient joint phenotype.

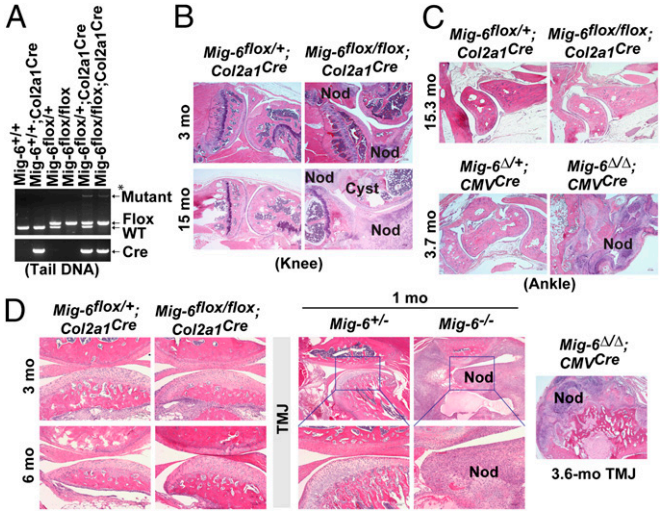

Fig. 3. Cartilage-specific deletion of *Mig-6* results in OA-like phenotype in the knee joints. (*A*) PCR genotyping of tail DNA from a *Mig-6*$^{flox/flox}$;*Col2a1*^{Cre} mouse and from control mice using the p5–p7–p8 triple primer combination. The p5–p8 primers detected the mutant allele, whereas the p7-p8 primers detected and distinguished floxed and WT alleles. *Note: Only a small population of cells in the tails expresses Col2a1 and thus Cre recombinase; floxed alleles were unmodified in the cells without Cre expression, resulting in PCR detection of a weak signal for the mutant allele together with a strong signal for the flox allele in the *Mig-6*$^{flox/flox}$;*Col2a1*^{Cre} tail. (*B*) Knee joints from *Mig-6*$^{flox/+}$;*Col2a1*^{Cre} mice and *Mig-6*$^{flox/flox}$;*Col2a1*^{Cre} mice at the indicated ages. (*C*) Ankles from *Mig-6*$^{flox/+}$;*Col2a1*^{Cre} and *Mig-6*$^{flox/flox}$;*Col2a1*^{Cre} mice at 15.3 mo, and from *Mig-6*$^{\Delta/+}$;*CMV*^{Cre} and *Mig-6*$^{\Delta/\Delta}$;*CMV*^{Cre} mice at 3.7 mo. (*D*) TMJs from *Mig-6*$^{flox/+}$;*Col2a1*^{Cre} and *Mig-6*$^{flox/flox}$;*Col2a1*^{Cre} mice at 3 and 6 mo, from *Mig-6*$^{+/-}$ and *Mig-6*$^{-/-}$ mice at 1 mo, and from a *Mig-6*$^{\Delta/\Delta}$;*CMV*^{Cre} mouse at 3.6 mo. Osteophytes are indicated by "Nod" and subchondral cysts by "Cyst".

Thickening of Articular Cartilage and an Increase of Chondrocytes in *Mig-6*$^{flox/flox}$;*Col2a1*^{Cre} Knees. To determine whether deletion of *Mig-6* in the chondrocyte affects the production of extracellular matrix in the knee joint, we used Safranin O staining to detect proteoglycans, a major ECM component in cartilage. We found that the thickness of articular cartilage that was positive for proteoglycans was much wider in the *Mig-6*$^{flox/flox}$;*Col2a1*^{Cre} knee than in the *Mig-6*$^{flox/+}$;*Col2a1*^{Cre} control knee, especially at older ages (Fig. 4*A*). The osteophytes formed in the *Mig-6*$^{flox/flox}$;*Col2a1*^{Cre} knee also synthesized an abundance of proteoglycans (Fig. 4*A*). Proteoglycan distribution was not significantly different in the growth plates of the *Mig-6*$^{flox/flox}$;*Col2a1*^{Cre} mice versus the growth plates of their control littermates (Fig. 4*A*). Also, more collagen II was detected across the articular cartilage in the *Mig-6*$^{flox/flox}$;*Col2a1*^{Cre} mice than in *Mig-6*$^{flox/+}$;*Col2a1*^{Cre} control mice, although no such difference was observed in their growth plates (Fig. 4*B*). The efficiency of cartilage specific deletion of Mig-6 was determined by immunohistochemical (IHC) staining of Mig-6 in the joint tissues. As shown in Fig. 4*C*, Mig-6 was detected in the surface layers of the articular cartilage and the adjacent cells in the *Mig-6*$^{flox/+}$;*Col2a1*^{Cre} knee joints (Fig. 4*C*), a pattern that is similar to what was observed in the Mig-6/lacZ reporter mice (Fig. 1). In contrast, we observed no Mig-6 expression in the chondrocytes in the articular cartilage and in the osteophytes of the *Mig-6*$^{flox/flox}$;*Col2a1*^{Cre} knee joints (Fig. 4*C*).

To further study *Mig-6*$^{flox/flox}$;*Col2a1*^{Cre} knees versus *Mig-6*$^{flox/+}$;*Col2a1*^{Cre} control knees, we took mice between 13.9 and 16.1 mo of age and compared their articular cartilage thicknesses. We found that the distance between the articular surface and the tidemark was much wider in the *Mig-6*$^{flox/flox}$;*Col2a1*^{Cre} femurs

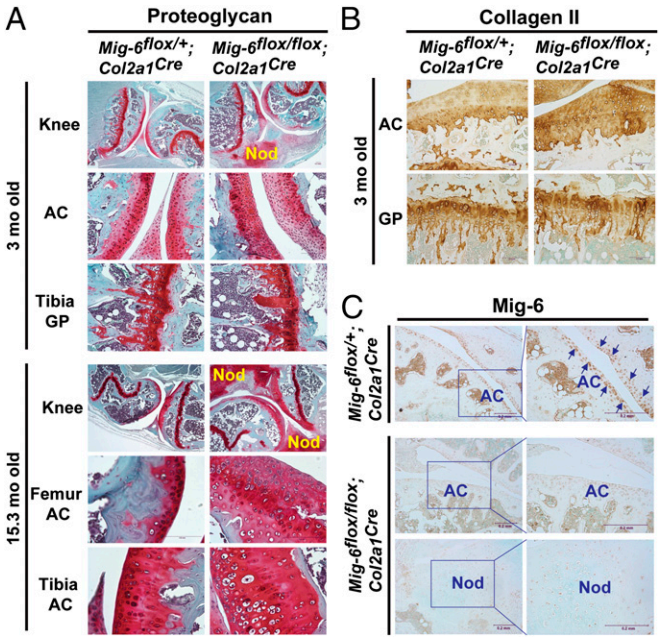

Fig. 4. Proteoglycan and collagen II distributions and detection of Mig-6 expression in the knee joints of *Mig-6$^{flox/flox}$;Col2a1^{Cre}* and the control mice. (*A*) Safranin O staining was used to detect proteoglycan in the knee joints of the *Mig-6$^{flox/+}$;Col2a1^{Cre}* and *Mig-6$^{flox/flox}$;Col2a1^{Cre}* mice at 3 and 15.3 mo of age. The osteophytes (labeled "nod") in the *Mig-6$^{flox/flox}$;Col2a1^{Cre}* joints at both ages produced an abundance of proteoglycans. The thickness of the proteoglycan-positive articular cartilage (AC) in both the femur and tibia was significantly increased in the *Mig-6$^{flox/flox}$;Col2a1^{Cre}* joints especially in older mice, relative to those of *Mig-6$^{flox/+}$;Col2a1^{Cre}*control joints. The distribution of proteoglycans in the growth plates (GP) of both strains appeared similar. (*B*) IHC staining of collagen II in the articular cartilage and growth plate of 3-mo-old *Mig-6$^{flox/+}$;Col2a1^{Cre}* and *Mig-6$^{flox/flox}$;Col2a1^{Cre}* knee joints. (*C*) Detection of Mig-6 expression in the *Mig-6$^{flox/+}$;Col2a1^{Cre}* and *Mig-6$^{flox/flox}$;Col2a1^{Cre}* knee joints by IHC staining. The arrows indicate representative positively stained cells.

and tibias (Fig. 5 *A* and *B*). Furthermore, the number of chondrocytes in the articular cartilage above the tidemark was two- to threefold higher in the *Mig-6$^{flox/flox}$;Col2a1^{Cre}* femurs and tibias than in control joints (Fig. 5*C*). These data indicate that deletion of *Mig-6* in the chondrogenic cells results in chondrocyte overproliferation in the articular cartilage, leading to its thickening and to increased production of proteoglycan and collagen II.

Osteophyte Development Resembles Endochondral Ossification. Besides the thickening of articular cartilage, the most prominent pathological change in mice having chondrocyte-specific deletion of Mig-6 was the development of osteophytes within the knee joints (see Figs. 3 and 4). To determine how these osteophytes formed, we used IHC staining of collagens type II and X, as well as the proliferative cell marker proliferating cell nuclear antigen (PCNA). In the middle zone of the osteophyte were hypertrophic chondrocytes that stained positive for collagen type X, surrounded by many collagen II-positive chondrocytes (Fig. 6 *A* and *B*). In the older mice, the regions in the inner zone surrounded by the hypertrophic chondrocytes appeared with no viable cells, but only matrix (Fig. 6*B*). These regions were likely undergoing mineralization, as previously observed in the osteophytes of *Mig-6$^{-/-}$* mice (11). PCNA staining showed proliferating cells at the edge of the osteophytes as well as around the articular cartilage in the *Mig-6$^{flox/flox}$;Col2a1^{Cre}* knee joint (Fig. 6*C*). The development of osteophytes in the *Mig-6$^{-/-}$* and *Mig-6$^{flox/flox}$;Col2a1^{Cre}* mice appears to resemble endochondral ossification, an important bone development process (24, 25).

Detection of Enhanced EGFR Signaling in the Mig-6–Deficient Chondrocytes. Mig-6 is known to be a negative regulator of the EGFR pathway in other tissues, so we asked whether EGFR signaling was affected by the deficiency of Mig-6 in the chondrocytes. We found that the chondrocytes in the superficial zone of articular cartilage as well as in the osteophytes of the *Mig-6$^{flox/flox}$;Col2a1^{Cre}* knee joint showed significantly elevated EGFR phosphorylation, which was hardly detected in the *Mig-6$^{flox/+}$;Col2a1^{Cre}* control knee (Fig. 6*D*). Furthermore, an increased phosphorylation of extracellular-signal-regulated kinase (ERK), a key signaling molecule downstream of EGFR, was also observed along with the elevated p-EGFR in those Mig-6–deficient chondrocytes in the *Mig-6$^{flox/flox}$;Col2a1^{Cre}* knee joint (Fig. 6*D*). Taken together, these data suggest that the joint disorder in mice with cartilage-specific deletion of Mig-6 might be due to overactivation of EGFR signaling in the chondrocytes in which Mig-6 is normally expressed.

Discussion

Mice with Mig-6 deficiency develop early-onset OA-like disorder in the synovial joints (11), as well as neoplasia in various tissues (8, 9). More effort has been made to understand the role of Mig-6 as a tumor suppressor in cancers, but studies of its role in joint homeostasis has been limited. Mig-6 is essential for maintaining the integrity of postnatal synovial joints, and loss of its activity leads to the formation of large osteophytes along with degradation of articular cartilage and subchondral cyst formation in the joints including knee, ankle, and TMJ (11).

How Mig-6 exerts its protective activity in the synovial joints and in what cells its activity is required are two fundamental questions. Addressing these questions will lead to a better understanding of the role of Mig-6 in the maintenance of joint homeostasis and in the pathogenesis of OA. In this study, we generated a *Mig-6/lacZ* reporter mouse strain that allows precise determination of when and in what cells *Mig-6* is expressed. The expression pattern of *Mig-6* in the joint turned out to be unique. A high level of β-galactosidase activity was detected in the cells

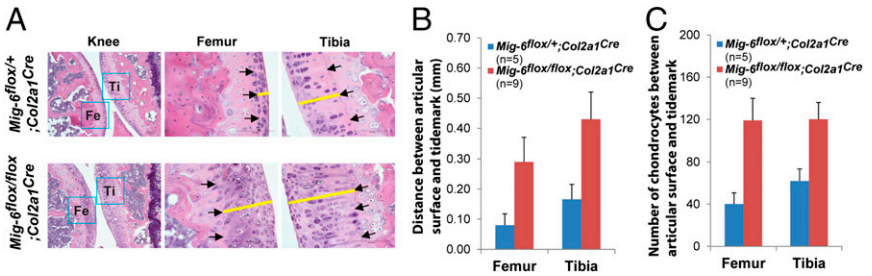

Fig. 5. Chondrocyte-specific deletion of Mig-6 resulted in thickening of articular cartilage accompanying increase of chondrocyte numbers. (*A*) Representative knee joints of the *Mig-6$^{flox/+}$;Col2a1^{Cre}* and *Mig-6$^{flox/flox}$;Col2a1^{Cre}* mice (age 16.1 mo) are shown. The arrows indicate the tidemarks, and the yellow bars measure the distance between the tidemark and the surface of the articular cartilage. (*B*) The distance between the articular surface and the tidemark is significantly increased in both femurs and tibias of *Mig-6$^{flox/flox}$;Col2a1^{Cre}* mice. (*C*) The number of chondrocytes in the articular cartilage between articular surface and tidemark (40× magnification fields) was also significantly increased in the *Mig-6$^{flox/flox}$;Col2a1^{Cre}* mice relative to their control mice (ages between 13.9 and 16.1 mo). The rectangles indicate the average values, and the error bars indicate the SD.

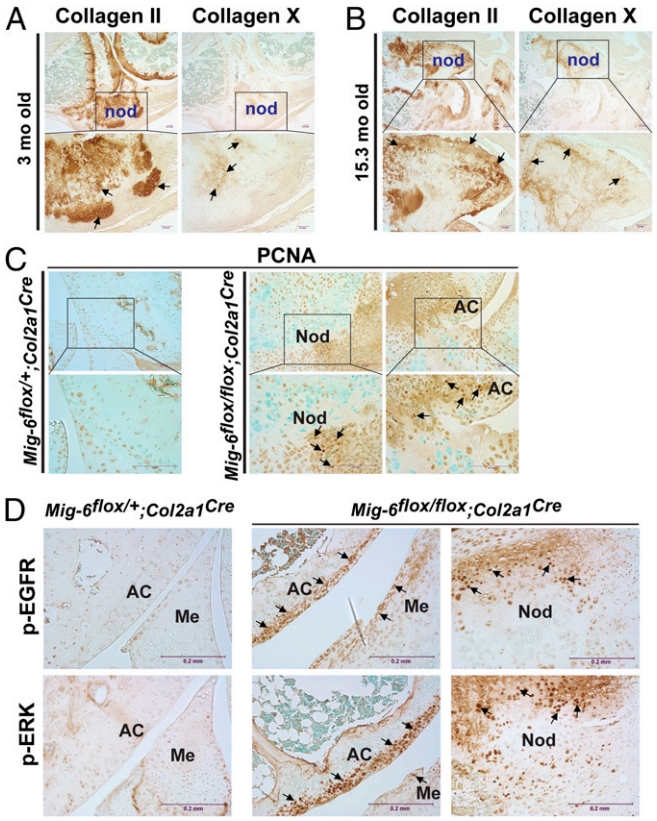

Fig. 6. Detection of collagens type II, type X, PCNA, p-EGFR, and p-ERK in the *Mig-6*$^{flox/flox}$;*Col2a1*^{Cre} knee joint. Strong staining of collagen II was detected within the osteophytes (labeled "nod") in both 3-mo-old (*A*) and 15.3-mo-old (*B*) knee joints. In the inner zones of the osteophytes were collagen X–positive hypertrophic chondrocytes surrounded by collagen II–positive chondrocytes. (*C*) Detection of proliferating cells in the osteophytes and articular cartilage by IHC staining of PCNA in knee joint sections derived from *Mig-6*$^{flox/+}$;*Col2a1*^{Cre} and *Mig-6*$^{flox/flox}$;*Col2a1*^{Cre} mice at 3 mo of age. The PCNA-positive cells were detected in osteophytes and around the articular cartilage (AC) in the *Mig-6*$^{flox/flox}$;*Col2a1*^{Cre} knee. (*D*) Detection of p-EGFR and p-ERK in the *Mig-6*$^{flox/+}$;*Col2a1*^{Cre} and *Mig-6*$^{flox/flox}$;*Col2a1*^{Cre} knee joints by IHC staining. The arrows indicate representative positively stained (brown) cells.

covering the entire surface of synovial joint cavity, including the chondrocytes in the superficial zone of articular cartilage and in the outer layer of meniscus, as well as the synovial lining cells (Fig. 1). These cells are required for in maintaining a healthy joint. We assume that this expression pattern can explain the OA-like phenotype developed in Mig-6–deficient joints, because the affected regions are where Mig-6 is expressed. Even though the osteoarthritic changes in Mig-6–deficient mice can be observed at about one month of age, a similar Mig-6 expression pattern is found in the prenatal day-16 embryonic joint. These data suggest that Mig-6 activity in these cells is intrinsic for the joints. The onset of the OA-like phenotype in Mig-6–deficient mice likely involves other postnatal factors, such as the mechanical stress on the joints in postnatal activities.

Knowing that Mig-6 is expressed in the chondrocytes of articular cartilage and the adjacent locations, we sought to determine what role chondrocytes might be playing in the onset and progression of OA-like disorder in *Mig-6*–deficient joints. A change in the behavior of chondrocytes in the articular cartilage is believed to play an important role during OA pathogenesis (18–20). We conditionally deleted *Mig-6* in the chondrogenic cells and, to our surprise, found that the joint phenotype only partially recapitulated the OA-like disorder of mice with complete deletion of *Mig-6*. Thus, deletion of Mig-6 in chondrocytes alone might not be sufficient for the onset of the disorder in the joints other than the knee, and other cell types must be involved in developing Mig-6–deficient OA-like phenotype in multiple synovial joints. The key to explaining this phenotypic difference likely lies in the meniscus, because the osteophytes formed in the knee were mostly close to or extended from the meniscus, whose surface chondrocytes display significant Mig-6 activity.

Osteophyte formation was the most profound pathological change observed in the knee joints of *Mig-6*$^{flox/flox}$;*Col2a1*^{Cre} mice. The osteophyte is a common pathological feature in OA and is one of the defining criteria for diagnosis in humans (26). The formation of osteophytes in Mig-6–deficient joints closely resembled endochondral ossification, a bone-development process especially important for long bone growth (24, 25). The osteophytes appeared at the edge of meniscus as newly formed cartilage rich in proteoglycans and collagens, followed by chondrocyte maturation, hypertrophy, and mineralization. The formation of osteophytes is likely the result of inappropriate cell proliferation in the absence of Mig-6; such proliferative activity was also seen around the articular cartilage. Recently, it was reported that specific deletion of Mig-6 in the limbs (*Mig-6–flox;Prx1*^{Cre} mice) results in a similar articular cartilage thickening and increased proliferation of chondrocytes (27). Mig-6 deficiency may also lead to defects in ECM remodeling by affecting the production of anabolic and catabolic factors as well as proteases from the chondrocytes, thereby affecting the health of the articular cartilage.

Another critical unanswered question is: what signaling pathway(s) is responsible for the onset and progression of the OA-like phenotype in Mig-6–deficient joints? The most well-established role for Mig-6 in cancer cells is as a negative feedback regulator of EGFR (3–6), and EGFR signaling is known to play an important role in bone development (28–31). TGF-α, one of the ligands for EGFR, has been reported to be increased in human osteoarthritic joints (32), and it can induce articular cartilage degradation in animal models (33, 34). EGFR signaling appears to be activated in the chondrocytes of the articular cartilage and in the osteophyte of the *Mig-6*$^{flox/flox}$;*Col2a1*^{Cre} knee joints (Fig. 6*D*). Therefore, it is possible that overactivation of EGFR signaling plays a role in the development of the OA-like disorder in the Mig-6–deficient joints.

In conclusion, our study demonstrates that Mig-6 is expressed in the cells across the entire surface of the synovial joints and that chondrocyte-specific deletion of Mig-6 results in a partial Mig-6–deficient OA-like phenotype. Our findings lay the groundwork for understanding the role of Mig-6 in the maintenance of joint homeostasis and in the pathogenesis of OA. Our findings also indicate the involvement of other cells in fully developing a Mig-6–deficient OA-like phenotype.

Materials and Methods

Generation of Mig-6/lacZ Reporter Mice. The pPNT vector (35) was used as a backbone for constructing the Mig-6/lacZ targeting vector. Briefly, a 5-kb genomic DNA fragment upstream of exon 2 and a 3-kb fragment downstream of exon 3 were inserted into the pPNT vector, serving as the 5′ and 3′ homologous recombination arms, respectively. Between the two recombination arms was a DNA cassette containing lacZ reporter (β-galactosidase), PGK-Neo, and exons 2 and 3 of the *Mig-6* gene, flanked by LoxP and FRT sequences. The lacZ reporter sequence was led by a splicing adaptor (SA) sequence derived from the junction of *Mig-6* intron 1 and exon 2, and followed by a SV40 poly-A signal. The targeting vector was confirmed by sequencing and linearized by unique NotI digestion for transfecting 129Sv embryonic stem (ES) cells by electroporation. After neomycin selection, positive ES clones were screened and used for generating Mig-6/lacZ reporter mice. The proper homologous recombination in the ES cells and mice was confirmed by PCR using Platinum PCR SuperMix High Fidelity (Invitrogen) and the primers listed in Table S1.

Generation of Mig-6–Floxed Mice. To construct the Mig-6 targeting vector, a 2.5-kb genomic DNA fragment downstream of the exon 4 was first inserted between the BamHI and EcoRI sites in the pPNT vector, and it served as the 3′ homologous recombination arm. Next, a *Mig-6* gene sequence containing exons 2–4 was flanked by an FRT and a LoxP sequence and was inserted into the XhoI and BamHI sites in the pPNT vector containing the 3′ recombination arm. Lastly, a DNA cassette containing a 5-kb *Mig-6* genomic DNA fragment upstream of the exon 2 (serving as the 5′ homologous recombination arm), a LoxP and a FRT sequence, and the PGK-Neo was constructed into the pBluescript II SK vector (Stratagene), and then transferred into the pPNT vector derivative between the NotI and XhoI sites. The resulted targeting vector was confirmed by sequencing and used for generating Mig-6–floxed ES cells and mice. The primers used for confirmation of proper homologous recombination and genotyping are listed in Table S1.

Sources of Other Mouse Strains. *Col2a1-Cre* transgenic mice, which express Cre recombinase under the control of the mouse type II collagen gene (*Col2a1*) regulatory regions (21); *CMV-Cre* transgenic mice, which express Cre under the control of a human cytomegalovirus minimal promoter (CMV) (23); and FLPeR mice (22) were all obtained from The Jackson Laboratory. The *Mig-6*$^{-/-}$ mice have been described (11). All mouse studies were approved by the Institutional Animal Care and Use Committee of Van Andel Research Institute.

PCR Genotyping and RT-PCR. For routine genotyping, genomic DNA was extracted from mouse tails, and PCR was performed using GoTaq Green Master Mix (Promega). For RT-PCR analysis, total RNA was extracted from mouse tissue using TRIzol reagent (Invitrogen), first-strand cDNA was synthesized from 1 μg of RNA using SuperScript II Reverse Transcriptase (Invitrogen), and then PCR amplification was performed using the following primer pairs: Mig6-F and Mig6-R for Mig-6, and Actin-F and Actin-R for mouse β-actin (see Table S1 for primer sequences).

Skeletal Preparation and Histology. Mouse limbs and skulls were harvested, trimmed to remove skin and soft tissues, fixed in formalin overnight, decalcified in Immunocal (Decal Chemical Corp) for a week at 4 °C, and embedded in paraffin. The formalin-fixed paraffin-embedded (FFPE) blocks were cut for preparation of 5-μm sections. The sections were stained with hematoxylin and eosin (H&E) for histological analyses. Safranin O staining was used for detection of proteoglycan in the cartilage.

Immunohistochemistry. The FFPE sections were deparaffinized and incubated in 0.5 M glacial acetic acid containing 0.1% pepsin for 2 h at 37 °C for antigen retrieval. The immunohistochemical staining was performed using a M.O.M. kit and a VECTASTAIN ABC kit, and was visualized using a DAB Peroxidase Substrate kit (Vector Laboratories). The primary antibodies used were antibodies against PCNA (Santa Cruz Biotechnology), collagen type II (Chemicon International), collagen type X (Quartett), Mig-6 (Proteintech), p-EGFR, and p-ERK (Cell Signaling). Sections were counterstained with Methyl Green. PCNA staining was done without antigen retrieval. For Mig-6, p-EGFR and p-ERK staining, antigen retrieval was done by incubating FFPE sections in Digest-All 1 (Ficin Solution; Invitrogen) for 10 min at 37 °C.

β-Galactosidase Staining. Embryos and limbs were embedded in optimal cutting temperature (OCT) compound on dry ice, and 5-μm frozen sections were prepared for β-galactosidase staining. Briefly, frozen sections were fixed for 5 min in PBS containing 2% (wt/vol) paraformaldehyde and 0.125% glutaraldehyde. The sections were stained at room temperature overnight in β-gal staining solution containing 5 mM $K_4Fe(CN)_6$, 5 mM $K_3Fe(CN)_6$, 1 mM $MgCl_2$, 0.01% sodium desoxycholate, 0.02% Nonidet P-40, and 2 mg/mL X-gal. After X-gal staining, the sections were counterstained with Nuclear Fast Red, mounted with mounting medium, and cover-slipped.

ACKNOWLEDGMENTS. We thank Bryn Eagleson and the vivarium staff for animal handling and care; Bree Berghuis, Lisa Turner, and Eric Hudson for histology assistance; Pamela Swiatek (Brown University) and Kellie Sisson (Michigan State University) for gene-targeting technique support; and David Nadziejka for critical reading and editing of the manuscript. We thank Kay Koo and Laura Holman for assisting manuscript preparation, and the Jay and Betty Van Andel Foundation for funding.

1. Zhang YW, Vande Woude GF (2007) Mig-6, signal transduction, stress response and cancer. *Cell Cycle* 6(5):507–513.
2. Zhang YW, Vande Woude GF (2013) MIG-6 and SPRY2 in the regulation of receptor tyrosine kinase signaling: Balancing act via negative feedback loops. *Future Aspects of Tumor Suppressor Gene*, ed Cheng Y (InTech, Rijeka, Croatia), pp 199–221.
3. Anastasi S, et al. (2003) Feedback inhibition by RALT controls signal output by the ErbB network. *Oncogene* 22(27):4221–4234.
4. Zhang X, et al. (2007) Inhibition of the EGF receptor by binding of MIG6 to an activating kinase domain interface. *Nature* 450(7170):741–744.
5. Frosi Y, et al. (2010) A two-tiered mechanism of EGFR inhibition by RALT/MIG6 via kinase suppression and receptor degradation. *J Cell Biol* 189(3):557–571.
6. Hackel PO, Gishizky M, Ullrich A (2001) Mig-6 is a negative regulator of the epidermal growth factor receptor signal. *Biol Chem* 382(12):1649–1662.
7. Makkinje A, et al. (2000) Gene 33/Mig-6, a transcriptionally inducible adapter protein that binds GTP-Cdc42 and activates SAPK/JNK. A potential marker transcript for chronic pathologic conditions, such as diabetic nephropathy. Possible role in the response to persistent stress. *J Biol Chem* 275(23):17838–17847.
8. Zhang YW, et al. (2007) Evidence that MIG-6 is a tumor-suppressor gene. *Oncogene* 26(2):269–276.
9. Ferby I, et al. (2006) Mig6 is a negative regulator of EGF receptor-mediated skin morphogenesis and tumor formation. *Nat Med* 12(5):568–573.
10. Jin N, et al. (2009) Mig-6 is required for appropriate lung development and to ensure normal adult lung homeostasis. *Development* 136(19):3347–3356.
11. Zhang YW, et al. (2005) Targeted disruption of Mig-6 in the mouse genome leads to early onset degenerative joint disease. *Proc Natl Acad Sci USA* 102(33):11740–11745.
12. Burton-Wurster N, et al. (2005) Genes in canine articular cartilage that respond to mechanical injury: Gene expression studies with Affymetrix canine GeneChip. *J Hered* 96(7):821–828.
13. Mateescu RG, Todhunter RJ, Lust G, Burton-Wurster N (2005) Increased MIG-6 mRNA transcripts in osteoarthritic cartilage. *Biochem Biophys Res Commun* 332(2):482–486.
14. Lawrence RC, et al.; National Arthritis Data Workgroup (2008) Estimates of the prevalence of arthritis and other rheumatic conditions in the United States. Part II. *Arthritis Rheum* 58(1):26–35.
15. Brandi ML, et al. (2001) Genetic markers of osteoarticular disorders: Facts and hopes. *Arthritis Res* 3(5):270–280.
16. van der Kraan PM (2012) Osteoarthritis year 2012 in review: Biology. *Osteoarthritis Cartilage* 20(12):1447–1450.
17. Loeser RF, Goldring SR, Scanzello CR, Goldring MB (2012) Osteoarthritis: A disease of the joint as an organ. *Arthritis Rheum* 64(6):1697–1707.
18. Buckwalter JA, Mankin HJ, Grodzinsky AJ (2005) Articular cartilage and osteoarthritis. *Instr Course Lect* 54:465–480.
19. Tchetina EV (2011) Developmental mechanisms in articular cartilage degradation in osteoarthritis. *Arthritis (Egypt)* 2011:683970.
20. Goldring MB (2000) The role of the chondrocyte in osteoarthritis. *Arthritis Rheum* 43(9):1916–1926.
21. Sakai K, et al. (2001) Stage-and tissue-specific expression of a Col2a1-Cre fusion gene in transgenic mice. *Matrix Biol* 19(8):761–767.
22. Farley FW, Soriano P, Steffen LS, Dymecki SM (2000) Widespread recombinase expression using FLPeR (flipper) mice. *Genesis* 28(3-4):106–110.
23. Schwenk F, Baron U, Rajewsky K (1995) A cre-transgenic mouse strain for the ubiquitous deletion of loxP-flanked gene segments including deletion in germ cells. *Nucleic Acids Res* 23(24):5080–5081.
24. Kronenberg HM (2003) Developmental regulation of the growth plate. *Nature* 423(6937):332–336.
25. Karsenty G, Wagner EF (2002) Reaching a genetic and molecular understanding of skeletal development. *Dev Cell* 2(4):389–406.
26. Altman R, et al.; Diagnostic and Therapeutic Criteria Committee of the American Rheumatism Association (1986) Development of criteria for the classification and reporting of osteoarthritis. Classification of osteoarthritis of the knee. *Arthritis Rheum* 29(8):1039–1049.
27. Shepard JB, Jeong JW, Maihle NJ, O'Brien S, Dealy CN (2013) Transient anabolic effects accompany epidermal growth factor receptor signal activation in articular cartilage in vivo. *Arthritis Res Ther* 15(3):R60.
28. Schneider MR, Sibilia M, Erben RG (2009) The EGFR network in bone biology and pathology. *Trends Endocrinol Metab* 20(10):517–524.
29. Zhu J, Shimizu E, Zhang X, Partridge NC, Qin L (2011) EGFR signaling suppresses osteoblast differentiation and inhibits expression of master osteoblastic transcription factors Runx2 and Osterix. *J Cell Biochem* 112(7):1749–1760.
30. Usmani SE, et al. (2012) Transforming growth factor alpha controls the transition from hypertrophic cartilage to bone during endochondral bone growth. *Bone* 51(1):131–141.
31. Zhang X, et al. (2011) The critical role of the epidermal growth factor receptor in endochondral ossification. *J Bone Miner Res* 26(11):2622–2633.
32. Hallbeck AL, Walz TM, Briheim K, Wasteson A (2005) TGF-alpha and ErbB2 production in synovial joint tissue: Increased expression in arthritic joints. *Scand J Rheumatol* 34(3):204–211.
33. Appleton CT, Usmani SE, Bernier SM, Aigner T, Beier F (2007) Transforming growth factor alpha suppression of articular chondrocyte phenotype and Sox9 expression in a rat model of osteoarthritis. *Arthritis Rheum* 56(11):3693–3705.
34. Appleton CT, Usmani SE, Mort JS, Beier F (2010) Rho/ROCK and MEK/ERK activation by transforming growth factor-alpha induces articular cartilage degradation. *Lab Invest* 90(1):20–30.
35. Tybulewicz VL, Crawford CE, Jackson PK, Bronson RT, Mulligan RC (1991) Neonatal lethality and lymphopenia in mice with a homozygous disruption of the c-abl proto-oncogene. *Cell* 65(7):1153–1163.